ENERGY AND EXERGY ANALYSES OF A COMBINED CYCLE POWER PLANT WITH INLET FUEL HEATING

Ting CHEN [1,2], Anping WAN [2*], Ke LI[1], Xingwei XIANG[1], Qinglong ZHOU[1], Qing ZUO[2], Liang ZHANG[3]

[1] State Key Laboratory of Fluid Power & Mechatronic Systems, Zhejiang University, Hangzhou 310027, China

[2] Mechanical and Electrical Department, Zhejiang University City College, Hangzhou, 310015, China

[3] Hangzhou Special Equipment Inspection Research Institute, Hangzhou, 310003, China

[*] Corresponding author; E-mail: wanap@zucc.edu.cn

By using exhaust gas as heating source, a combined cycle power plant with inlet fuel heating is investigated experimentally. Energy analysis and exergy analysis are carried out under different power load and ambient temperature. The results reveal that the thermal efficiency of the power plant system increases as power load increases. The thermal efficiency and power output at 5 ℃ are 54.15% and 412 MW, respectively; while when the ambient temperature is 35 ℃, the thermal efficiency and power output are 52.3% and 330 MW, respectively. Under the same conditions, the combustion chamber has the highest irreversibility rate, while the air compressor has the lowest. The irreversibility rate of the power plant system increases in line with power load. The second-law efficiency increases from 37.08% to 50.12% when the power load changes from 30% to 100%.

Keywords*: Combined cycle power plant, Power load, Efficiency, Exergy*

1. Introduction

According to a survey of the International Energy Agency in 2019, the global energy demand is predicted to rise by 30% in 2040, and over 20% of electricity generation fueled by natural gas [1]. A combined cycle power plant (CCPP) can utilize waste heat of exhaust from gas turbine to generate steam. And the steam enters into steam turbine to produce extra work The efficiency of the CCPP system is much higher than that of gas turbine cycle or the Rankine cycle [2]. Hence the CCPP systems have been developed rapidly [3-6].

Performance investigation on the normal CCPP systems have been carried out actively [7,8]. Aliyu et al. [9] presented the thermodynamic analysis of a CCPP system using design data. They revealed that the exergy efficiency of the turbine is the highest in the steam turbine cycle while the exergy efficiency of the condenser is the lowest one. Günnur Şen et al. [10] studied the effect of ambient temperature on electric power generation in a CCPP system using natural gas as fuel. The results showed that the efficiency of the components in the CCPP system decreased with increasing ambient temperature. And the electricity generation at ambient temperature of 8 ℃ was 227.7 MW, which is 30.4 MW higher than that of 23 ℃. And similar results have been reported in many studies

that the power output of CCPP system decreases considerably with increasing ambient temperature [11-15].

A lot of effort has been done to improve the performance of gas-fired power plants, since most gas-fired power plants are large-scaled, and even a small improvement in efficiency can lead to a huge amount of power gain [16]. Ibrahim et al. [17] investigated the performance of a gas turbine-based power plant under different air supply temperature. They revealed that the overall system efficiency can be significantly increased by reducing the inlet air temperature. Mahapatra and Sanjay [18] investigated a CCPP system with inlet air cooling using second-law thermodynamics. And they revealed that the overall exergy of the system can be increased by using inlet air cooling system. Kotowicz et al. [19] investigated the thermodynamic and economic characteristics of a CCPP with gas turbine steam cooling. They found that the utilization of heat from the compressed air in gas turbine was effective, and the use of steam as a coolant in the gas turbine improved its efficiency. Besides, Kotowicz and Brzęczek [20] also investigated the thermodynamic performance of various gas turbine improvements in CCPP system under different air-cooled cooling modes. The results showed that the efficiency of the CCPP system can be improved by using air-cooled cooling in the gas turbine and used its heat in the steam cycle. Kwon et al. [21] numerically analyzed the performance improvement of a CCPP system by dual cooling of the inlet air and turbine coolant. A lithium-bromide/water absorption chiller was integrated with the gas turbine. The results revealed that the power generation of the integration system was estimated to be 8.2% higher than the ordinary CCPP system.

The main contributions of the present study are:

Firstly, a CCPP system with inlet fuel heating (CCPP-IFH) is experimentally investigated. The natural gas is heated in a heater before it enters the combustion chamber, and the heating source of the heater is the flue gas.

Secondly, the CCPP-IFH system is tested under different part-load conditions and ambient temperatures. The experimental results can provide reference for further numerical investigation on CCPP system.

Thirdly, the energy and exergy analysis on the whole system and each component are performed on the basis of the actual operating data from the Banshan power plant in Hangzhou, China.

2. System description

In this study, a CCPP system with inlet fuel heating is established and tested. The experimental data are collected under different power load and weather conditions. This CCPP-IFH system is located in Hangzhou city (120 ^{o}E, 29 ^{o}N), China. The CCPP system consists of a PG9351FA turbine that produced by General Electric, a triple pressure heat recovery steam generator (HRSG), a D10 steam turbine, and a 390H Hydrogen-cooled generator. The schematic of the CCPP is shown in Fig. 1. Solid particles of dust and impurities in the ambient air are filtered through an air filter, and then enters the compressor. The natural gas that heated in the heater meets the compressed air in the combustion chamber, where fuel combustion takes place. Then combustion gases are expanded in the turbine to generate work. Part of the generated driving force is used to run the air compressor, and the left is used to generate electric power. The internal energy contained in the flue gas is recovered to run steam turbines.

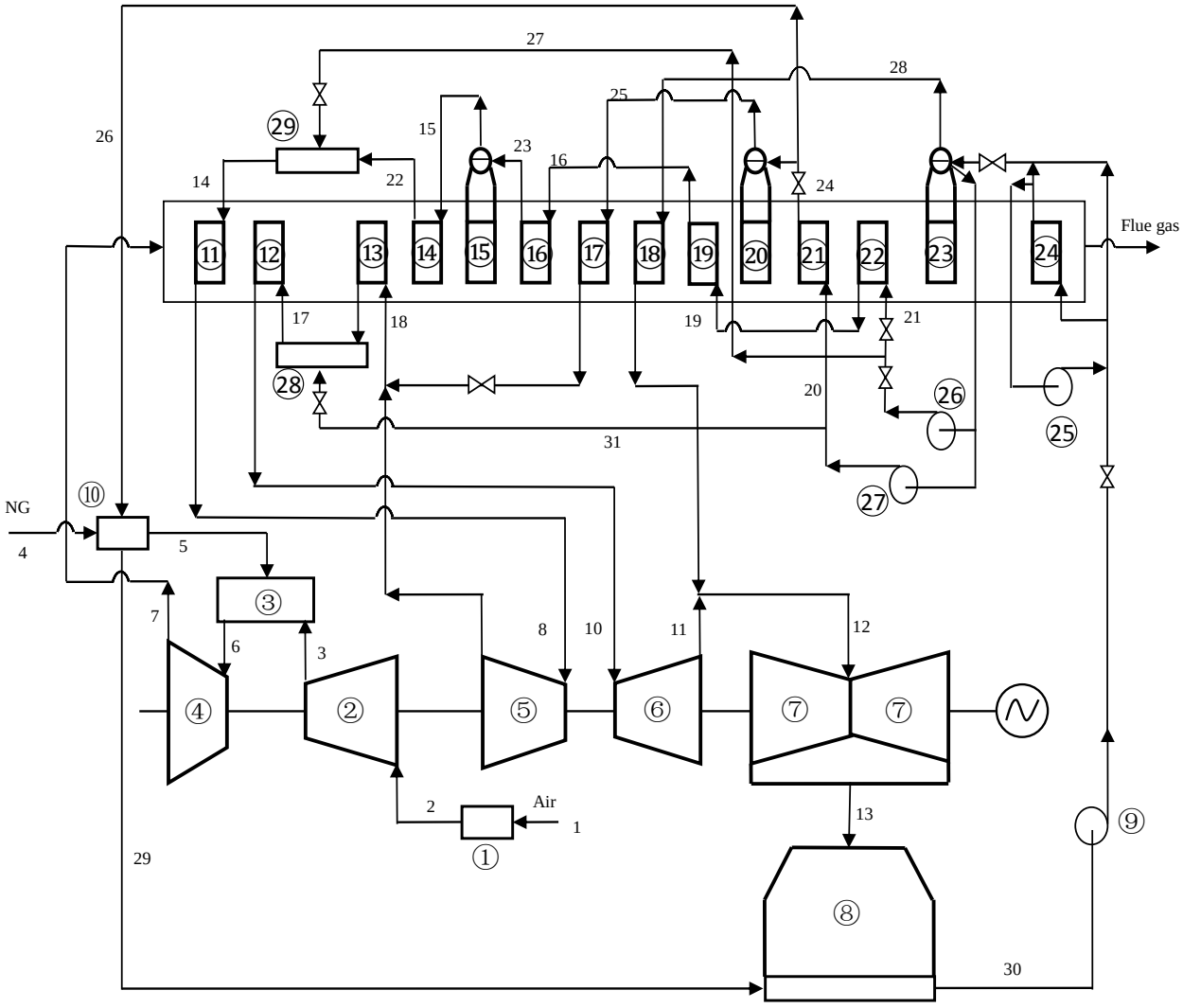

①Filter; ②Air compressor; ③Combustion chamber; ④Turbine; ⑤High pressure gas turbine; ⑥Intermediate pressure gas turbine; ⑦Low pressure gas turbine; ⑧Condenser; ⑨ ㉕ ㉖ ㉗ Recirculation pump; ⑩Heater; ⑪ ⑭ ⑰ ⑱Superheater; ⑫ ⑬Reheater; ⑮ ⑳ ㉓Evaporator; ⑯ ⑲ ㉑ ㉒ ㉔Economizer; ㉘ ㉙Desuperheater.

Fig. 1 Schematic diagram of the CCPP with inlet fuel heating system

Table 1. Raw data from the Banshan combined cycle power plant

Parameter	value							
Air mas flow rate (10^3kg/h)	2410	2360	2303	2270	2210	2135	2110	1968
Inlet air temperature (℃)	5	10	15	17.5	20	25	30	35
Fuel mass flow rate (10^3kg/h)	53	51	50.8	50.1	49.2	47.8	45.7	44.2
Flue gas mass flow rate (kg/h)	2479	2407	2364	2330	2303	2177	2100	2088
Flue gas outlet temperature (℃)	81.8	82.9	84.1	83.8	84.2	84.6	85.2	85.6
Turbine outlet temperature (℃)	590.9	600.7	604.8	607.1	613.5	618	620	623
Turbine outlet temperature (kPa)	105.9	105.2	104.7	104.4	104	102.9	102.8	100.8

The data are collected through a PIS (Plant information System), which is intergrated in the power plant system. The ambient temperature and pressure measurement uncertainty is ±0.05 K and ±0.13%. The uncertainties of the temperature, pressure and power output measurement in the system are ±2 K, 0.5%, and ±1%, respectively. The uncertainties of the calculated value are calculated by using the EES (Engineering Equation Solver) program. Some measured data are displayed in Table 1.

3. Analysis method

3.1. Energy analysis

The calculation of the CCPP system is performed by using EES program. The calculation is conducted according to the following two assumptions: (1) The natural gas burns completely in the combustion chamber; (2) No energy loss to the surroundings; (3) Kinetic and potential energies are negligible; (4) Kinetic and potential exergies are negligible.

Gas turbine:

The gas turbine consists of an air compressor, a combustion chamber and a turbine. The clean filtered ambient air enters the air compressor. The compressor outlet temperature was calculated by:

$$T_2 = T_1[1 + \frac{1}{\eta_{AC}}(r_{AC}^{\frac{n-1}{n}} - 1)], \tag{1}$$

where n is the ratio of specific heat:

$$n = \frac{c_{p,a}}{c_{v,a}}. \tag{2}$$

The specific heat at constant pressure was calculated as [22]:

$$c_p = 1.0481 - \frac{3.83719 \cdot T}{10^4} + \frac{9.45378 \cdot T^2}{10^7} - \frac{5.49031 \cdot T^3}{10^{10}} + \frac{7.92981 \cdot T^4}{10^{14}}. \tag{3}$$

The specific heat at constant volume was calculated by using EES program.

And the power balance in the compressor is:

$$\dot{W}_{AC} = (\dot{m}_a \cdot c_{p,3} \cdot T_3 - \dot{m}_a \cdot c_{p,2} \cdot T_2)/\eta_{AC}, \tag{4}$$

η_{AC} is the mechanical efficiency of the air compressor, $\dot{m}_a$, c_p and T are the mass flow rate, specific heat and temperature of the air, respectively.

The outlet pressure is calculated by:

$$P_3 = P_2 \cdot r_{AC}, \tag{5}$$

where r_{AC} is the pressure ratio.

The combustion process in the combustion chamber can be described as:

$$\dot{m}_a \cdot c_{p,3} \cdot T_3 + \eta_{CC} \cdot \dot{m}_{NG} \cdot LHV_{NG} + \dot{m}_{NG} \cdot c_{p,5} \cdot T_5 = \dot{m}_f \cdot h_6, \tag{6}$$

$$\dot{m}_a + \dot{m}_{NG} = \dot{m}_f. \tag{7}$$

The specific heat of the combustion gas can be calculated as [23]

$$c_{p,f} = 1.0888 - \frac{1.4159 \cdot T}{10^4} + \frac{1.916 \cdot T^2}{10^7} - \frac{1.24 \cdot T^3}{10^{10}} + \frac{3.067 \cdot T^4}{10^{14}}. \tag{8}$$

The high-pressure exhaust gas enters the turbine to produce power. The power produced by the turbine is:

$$\dot{W}_{TB} = \dot{m}_f \cdot (h_6 - h_7) \cdot \eta_{TB}. \quad (9)$$

Part of the power generated by the gas turbine is used to drive the air compressor, then the net power produced from the gas turbine is:

$$\dot{W}_{net} = \dot{W}_{TB} - \dot{W}_{AC}. \quad (10)$$

HRSG:

The triple pressure HRSG system is used to improve the energy utilization efficiency by recover the waste heat. The exhaust gas is used to heat feed water into steam with pressure of 9.563 MPa, 2.146 MPa and 0.366 MPa, respectively. Another steam line of the HRSG is connected to the heater, and the natural gas is heated to 185 ℃. The energy balance of the HRSG can be expressed as:

$$\dot{m}_7 \cdot h_7 + \dot{m}_9 \cdot h_9 + \dot{m}_{30} \cdot h_{30} - \dot{m}_8 \cdot h_8 - \dot{m}_{10} \cdot h_{10} - \dot{m}_{34} \cdot h_{34} - \dot{m}_{26} \cdot h_{26} - \dot{m}_{32} \cdot h_{32} = 0. \quad (11)$$

Steam turbine:

The energy balance of steam turbine can be calculated as:

$$\dot{W}_{ST} = \dot{m}_8 \cdot h_8 + \dot{m}_{10} \cdot h_{10} + \dot{m}_{12} \cdot h_{12} - \dot{m}_9 \cdot h_9 - \dot{m}_{11} \cdot h_{11} - \dot{m}_{13} \cdot h_{13}. \quad (12)$$

Condenser and natural gas heater:

The energy balance of the condenser and the natural gas heater can be expressed as:

$$\dot{m}_{13} \cdot h_{13} + \dot{m}_{29} \cdot h_{29} = \dot{m}_{30} \cdot h_{30}, \quad (13)$$

$$\dot{m}_4 \cdot (h_5 - h_4) = \dot{m}_{26} \cdot (h_{26} - h_{29}). \quad (14)$$

Thermal efficiency:

The thermal efficiency is defined as the ratio of the output to the input. The thermal efficiency of the GT, HRSG and the overall CCPP system is calculated as:

$$\eta_{I,\ GT} = \frac{\dot{W}_{net}}{\dot{m}_{NG} \cdot LHV}, \quad (15)$$

$$\eta_{I,\ HRSG} = \frac{T_7 - T_{34}}{T_7 - T_0}, \quad (16)$$

$$\eta_{I,\ CCPP} = \frac{\dot{W}_{net} + \dot{W}_{ST}}{\dot{m}_{NG} \cdot LHV}. \quad (17)$$

3.2. Exergy analysis

Exergy is defined as the useful work potential of a given amount of energy at some specified state. For this study, the work potential of the energy contained in the components of the CCPP system is investigated under normal operating conditions. And the amount of potential and kinetic exergy in CCPP system are too small, so they are neglected in the following analysis [24]. For any component of the system, the exergy conservation is expressed as:

$$\dot{I} = \dot{X}_{in} - \dot{X}_{out} - \Delta\dot{X}_{sys}. \quad (18)$$

The irreversibility rate $\dot{I}$, which is equivalent to the exergy destroyed, represents the energy that could have been converted to output but was not. And $\dot{X}_I$ and $\dot{X}_O$ are input and output exergy

flow rate. The exergy flow rate is defined as the exergy in the rate form. As mentioned previously, the kinetic and potential exergies are negligible, the exergy flow rates at different nodes is expressed as:

$$\dot{X}_N = \dot{m}_N \left\{ (h_N - h_0) - \left[\frac{(c_{p,N} + c_{p,0})}{2} \cdot \ln \frac{T_N}{T_0} - R \cdot \ln \frac{P_N}{P_0} \right] \right\}. \tag{19}$$

where R is the gas constant, the subscript 0 indicates the dead point. For different gases, the gas constant was determined from

$$R = \frac{R_u}{M}. \tag{20}$$

where R_u is the universal gas constant and M is the molar mass of the gas.

The thermal efficiency is defined on the basis of the first law of the thermodynamics. However, it makes no reference to the maximum possible performance. To overcome this deficiency, we need to analyze the second-law efficiency, which is expressed as:

$$\eta_{\text{II}} = 1 - \frac{\dot{\text{I}}}{\dot{X}_{in}}. \tag{21}$$

The irreversibility rate and the second-law efficiency in the components of the system can be expressed as bellows.

Air compressor:

$$\dot{I}_{AC} = \dot{X}_2 + \dot{W}_{AC} - \dot{X}_3, \tag{22}$$

$$\eta_{\text{II},\ AC} = 1 - \frac{\dot{I}_{AC}}{\dot{W}_{AC} + \dot{X}_2}. \tag{23}$$

Combustion chamber:

$$\dot{I}_{CC} = \dot{X}_3 + \dot{X}_5 - \dot{X}_6, \tag{24}$$

$$\eta_{\text{II},\ CC} = 1 - \frac{\dot{I}_{CC}}{\dot{X}_3 + \dot{X}_5}, \tag{25}$$

Where $\dot{X}_5$ can be calculated as:

$$\dot{X}_5 = \xi \cdot \dot{m}_{NG} \cdot LHV, \tag{26}$$

where ξ is 1.06 [25].

Since the air compressor is connected to the turbine by a shaft, it is drove by the work that produced by the turbine. In the study of Wang et al. [26], the energy consumed by the air compressor is neglected, however, according to the practical experience of CCPP system, the energy consumed by the air compressor may account for up to 30% of the total mechanical energy that generated by the turbine [26]. Then the irreversibility rate and second-law efficiency of the turbine is expressed as:

$$\dot{I}_{TB} = \dot{X}_6 - \dot{W}_{AC} - \dot{W}_{GT} - \dot{X}_7, \tag{27}$$

$$\eta_{\text{II},\ TB} = 1 - \frac{\dot{I}_{TB}}{\dot{X}_6}. \tag{28}$$

HRSG:

$$\dot{I}_{HRSG} = \dot{X}_7 + \dot{X}_9 + \dot{X}_{30} - \dot{X}_8 - \dot{X}_{10} - \dot{X}_{32} - \dot{X}_{33} - \dot{X}_{34}, \tag{29}$$

$$\eta_{\mathrm{II},\ HRSG} = 1 - \frac{\dot{I}_{HRSG}}{\dot{X}_7 + \dot{X}_9 + \dot{X}_{30}}. \tag{30}$$

Steam turbine:

$$\dot{I}_{ST} = \dot{X}_8 + \dot{X}_{10} + \dot{X}_{12} - \dot{X}_9 - \dot{X}_{11} - \dot{X}_{13} - \dot{W}_{GT}, \tag{31}$$

$$\eta_{\mathrm{II},\ ST} = 1 - \frac{\dot{I}_{ST}}{\dot{X}_8 + \dot{X}_{10} + \dot{X}_{12}}. \tag{32}$$

Condenser

$$\dot{I}_{Cond} = \dot{X}_{29} + \dot{X}_{13} - \dot{X}_{30}, \tag{33}$$

$$\eta_{\mathrm{II},\ Cond} = 1 - \frac{\dot{I}_{Cond}}{\dot{X}_{13} + \dot{X}_{29}}. \tag{34}$$

And the overall irreversibility rate and the second-law efficiency of the CCPP system is:

$$\dot{I}_{CCPP} = \dot{X}_1 + \dot{X}_4 - \dot{X}_{34} - \dot{W}_{GT} - \dot{W}_{ST}, \tag{35}$$

$$\eta_{\mathrm{II},\ CCPP} = 1 - \frac{\dot{I}_{CCPP}}{\dot{X}_1 + \dot{X}_4}. \tag{36}$$

Uncertainty analysis of the calculated value can be conducted according to Eq.(37),

$$\delta f = \sqrt{(\frac{\partial f}{\partial x})^2 \delta x + (\frac{\partial f}{\partial y})^2 \delta y + (\frac{\partial f}{\partial z})^2 \delta z}. \tag{37}$$

4. Results and discussion

4.1. Energy analysis results

In this section, the energy analysis results are displayed. By using the previously introduced uncertainty analysis equation, the errors of the thermal efficiencies are within ±1%. Fig. 2 and 3 show the thermal efficiency variations with power load and ambient temperature. The thermal efficiency of the HRSG changes slightly with power load conditions. The GT thermal efficiency and the CCPP-IFH system thermal efficiency increase linearly with power load conditions. The GT thermal efficiency increases by 85.1%, while CCPP-IFH increases by 35.2% when power load increases from 30% to 100%. The reason is that when the system is operated under partial power load, the air and fuel mass flow rates are reduced, then the work produced by the turbine is reduced, but the rotation speed

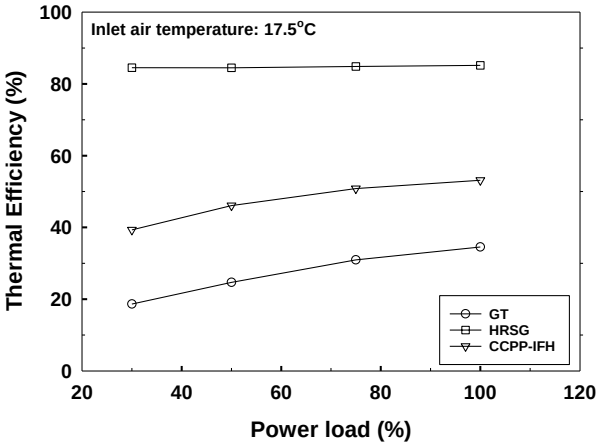

Fig. 2 Thermal efficiency with power load

of the AC is independent with the power load, which means that the work consumed by the AC is almost constant.

The thermal efficiency of HRSG almost maintains stable with changing ambient temperature. When the ambient temperature changes from 5 ℃ to 35 ℃, the GT thermal efficiency decreases from 36.3% to 34%. And the thermal efficiencies of the CCPP-IFH system at 5 ℃ and 35 ℃ are 54.15% and 52.3%, respectively. The reason is that the density of air is decreased with the increase in ambient temperature. Therefore, the mass flow rate of air that enters the air compressor decreases with increasing inlet air temperature.

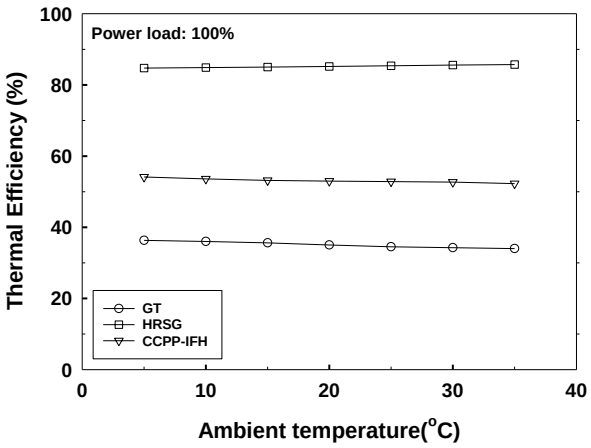

Fig. 3 Thermal efficiency with ambient temperature

4.2. Exergy analysis results

By using the previously introduced uncertainty analysis equation, the errors of the irreversibility rates and second-low efficiencies are within ±1%. Fig. 4 shows the irreversibility rate of the main components with power load. The irreversibility rate that generated in the AC is the lowest, and the CC contributes the highest irreversibility rate. At the power load of 100%, the irreversibility rate in the CC is 176.38 MW, it is 54.6% higher than that in the TB, 2.3 times of that in the HRSG, and almost 30 times of that in the AC. It is clear that the increase in irreversibility rates for CC, TB and HRSG are caused by the increase in air and fuel mass flow rates. For the AC, the increases in mass flow rates of air and fuel are almost entirely coverted to reversible work.

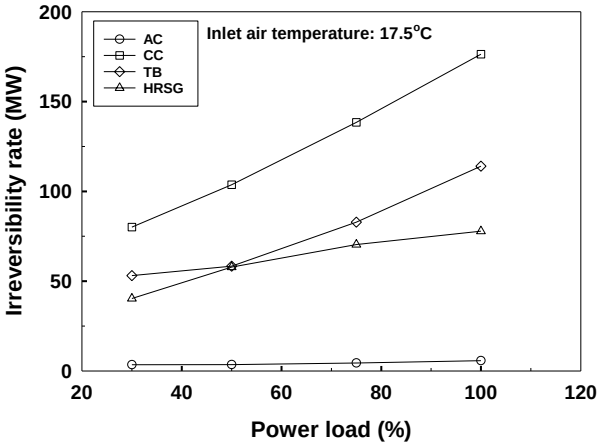

Fig. 4 Irreversibility rate of the main components with power load

The irreversibility rates of the main components at different ambient temperatures are presented in Fig. 5. The irreversibility rate in the AC is the lowest, while the highest is in the CC. The irreversibility rates in the AC, TB and the HRSG change slightly under different ambient temperatures. However, it decreases considerably in CC when the ambient temperature is changed 5 ℃ to 35 ℃. More specifically, it decreases by 17.2%. The reason for this decrease is that higher ambient temperature leads to higher temperature at CC inlet, and this is helpful for the combustion process.

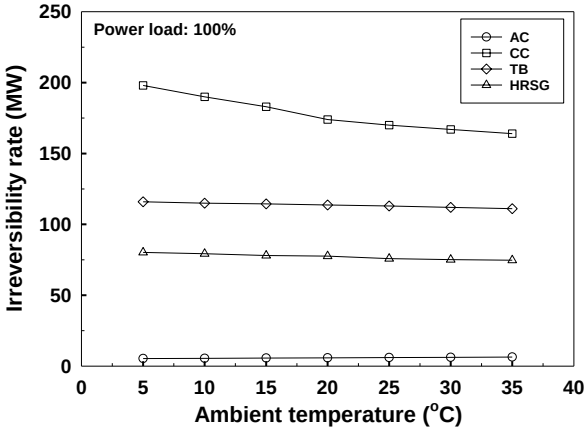

Fig. 5 Irreversibility rate of the main components with ambient temperature

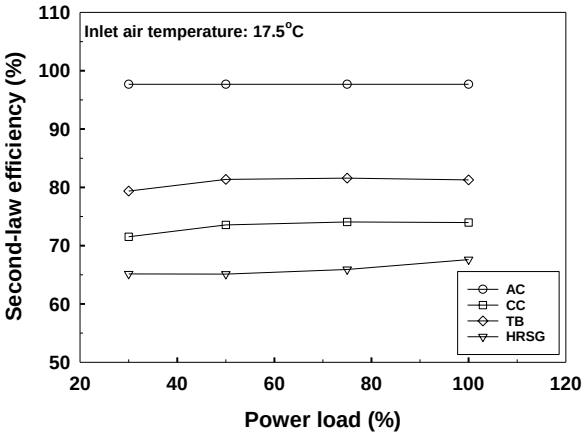

Fig. 6 Second-law efficiency of the main components with power load

The second-law efficiency variations of the main components with power load are shown in Fig. 6. The AC has the highest second-law efficiency with 97%, and it almost kept constant with the variation of the power load. The HRSG has the lowest second-law efficiency, it increases slightly with the increasing power load. When the power load increases from 30% to 100%, the second-law efficiency of the HRSG increases from 65.15% to 67.6%. The second-law efficiency of the CC also increases with the power load, it increases from 71.54% to 73.97%.

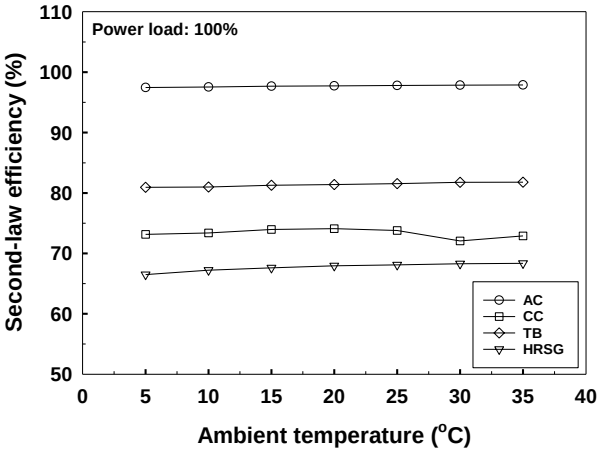

Fig. 7 Second-law efficiency of the main components with ambient temperature

Fig. 7 shows the second-law efficiency variation with ambient temperatures. The results show that the second-law efficiency for each component changes slightly with ambient temperatures. The second-law efficiency of the AC, TB and HRSG reach their highest values when the ambient temperature is 35 ℃. However, the second-law efficiency of CC reaches the highest value when the ambient temperature is 20 ℃.

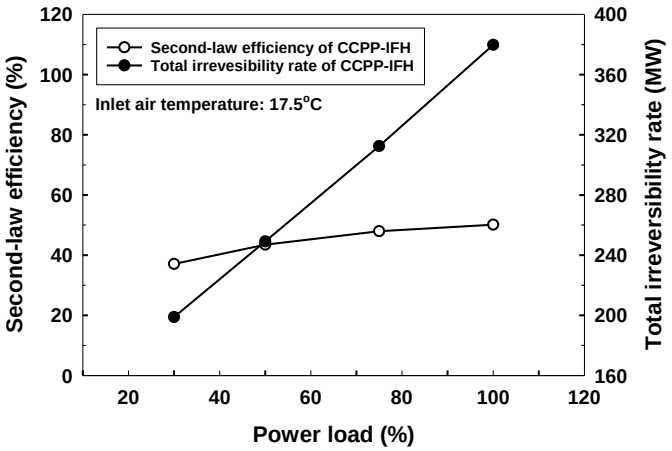

Fig. 8 Second-law efficiency and total irreversibility of the CCPP-IFH system with power load

Fig. 8 and Fig. 9 show the second-law efficiency and irreversibility rate of the CCPP-IFH system under different power load and ambient temperatures. The irreversibility rate of the system changes in line with power load. The second-law efficiency of the whole system increases from 37.08% to 50.12% when the power load changes from 30% to 100%. The irreversibility rates at 5 ℃ and 35 ℃ are 393.59 MW and 353.03 MW, respectively. The main reason is that the entropy increment, which accounts for part of the

irreversibility rate, increases as ambient temperature increases. Since the total exergy output under low ambient temperature is higher compared to that under high ambient temperature, the second-law efficiency increases slightly.

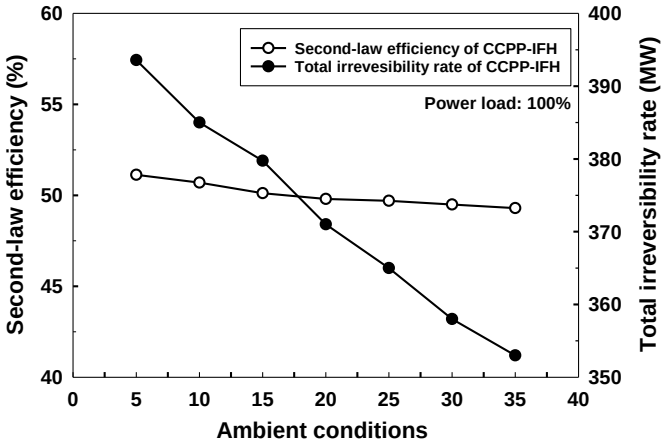

Fig. 9 Second-law efficiency and total irreversibility of the CCPP-IFH system with ambient temperature

5. Conclusions

In this study, a combined cycle power plant with inlet fuel heating (CCPP-IFH) system is proposed and studied experimentally. The intake natural gas is heated by the recovered energy in the HRSG to increase the system performance. The energy analysis and exergy analysis are proceeded under different power load and ambient temperatures. According to the results obtained from the performance analysis of the system, conclusions are summarized:

(1) The thermal efficiency of the CCPP-IFH system increases as power load increases since the work consumed by the AC is almost constan. The ambient temperature has a considerable impact on the thermal efficiency of the system. The main reason is that the air and fuel inputs are reduced with increasing ambient temperature.

(2) Under the same ambient temperature and power load condition, CC has the highest irreversibility rate, while AC has the lowest. The irreversibility rate of the CCPP-IFH system can be considerably improved if the CC is well modified.

(3) Under the same ambient temperature and power load condition, AC has the highest second-law efficiency, while HRSG has the lowest. The second-law efficiency of each component changes slightly with power load and ambient temperatures.

(4) The irreversibility rate of the CCPP-IFH system increases linearly with power load. The irreversibility rate of the CCPP-IFH system reaches the highest value when the ambient temperature is 5 ℃, and the second-law efficiency increases slightly when the ambient temperature change from 5 ℃ to 35 ℃.

Acknowledgment

This research is financially supported by National Natural Science Foundation of China (51705455), Aviation Science Foundation(20183333001) and China Postdoctoral Science Foundation funded project (2018T110587), Scientific Research Foundation of Zhejiang University City College(J-202113), Key Projects of Hangzhou Agricultural and Social Development Research Program (20212013B04）, Zhejiang Province Basic Public Welfare Research Project (LGG20E050007).

Nomenclature

AC	air compressor [-]
CC	combustion chamber [-]
CCPP	combined cycle power plant [-]
Cond	condenser [-]
c_p	specific heat at constant pressure[kJ $kg^{-1}k^{-1}$]
c_v	specific heat at constant volume[kJ $kg^{-1}k^{-1}$]
GT	gas turbine [-]
h	specific enthalpy [kJ kg^{-1}]
HRSG	heat recovery steam generator [-]
HT	high pressure steam turbine [-]
$\dot{I}$	irreversibility rate [MW]
IFH	inlet fuel heating [-]
IH	intermediate pressure steam turbine [-]
n	ratio of specific heat [-]
N	node number [-]
LHV	lower heating value [kJ kg^{-1}]
LH	low pressure steam turbine [-]
$\dot{m}$	mass flow rate [kg s^{-1}]
P	power output [MW]
r	pressure ratio [-]
ST	steam turbine [-]
T	temperature [℃]
$\dot{W}$	work/power output [MW]
$\dot{X}$	exergy flow rate [MW]

Greek symbols

η	efficiency [%]
η_I	thermal efficiency [%]
η_{II}	second-law efficiency [%]
ξ	the coefficient of fuel exergy [-]

Superscripts

a	air
f	flue gas
in	inlet
NG	natural gas
out	outlet
sys	system

References

[1] IEA. World energy outlook 2017. Organization for economic co-operation and development (2017).

[2] Jonsson, M., Yan, J., Humidified gas turbines—a review of proposed and implemented cycles. *Energy, 30 (2005),* pp. 1013-1078.

[3] Ibrahim, T. K., *et al.*, The optimum performance of the combined cycle power plant: A comprehensive review. *Renewable and Sustainable Energy Reviews,* 79, pp.459-474(2017).

[4] Bălănescu, D., Homutescu, V., Performance analysis of a gas turbine combined cycle power plant with waste heat recovery in Organic Rankine Cycle. *Procedia Manufacturing,* 32 (2019), pp.520-528.

[5] Pichardo, P. A., *et al.*, Techno-economic analysis of an intensified integrated gasification combined cycle (IGCC) power plant featuring a combined membrane reactor - adsorptive reactor (MR-AR) system, *Industrial and Engineering Chemistry Research,* 59(2020), 6, pp. 2430-2440.

[6] Boretti, A., Al-Zubaidy, S., A case study on combined cycle power plant integrated with solar energy in Trinidad and Tobago, *Sustainable Energy Technologies and Assessments,* 32 (2019), pp. 100-110.

[7] Alus, M., *et al.*, Optimization of the triple-pressure combined cycle power plant, Thermal Science, 16 (2012), 3, pp. 901-914.

[8] Xu, C., *et al.*, Performance improvement of a 330MW power plant by flue gas heat recovery system, *Thermal Science*, 20 (2014), pp.99-99.

[9] Aliyu, M., *et al.*, Energy, exergy and parametric analysis of a combined cycle power plant. *Thermal Science and Engineering Progress,* 15 (2020), pp. 100450.

[10] Şen, G., *et al.*, The effect of ambient temperature on electric power generation in natural gas combined cycle power plant—A case study. *Energy Reports,* 4 (2018), pp. 682-690.

[11] Garcia, S. I., *et al.*, Critical review of the first-law efficiency in different power combined cycle architectures, *Energy Conversion and Management,* 148 (2017), pp. 844–859.

[12] Moon, S. W., *et al.*, A novel coolant cooling method for enhancing the performance of the gas turbine combined cycle. *Energy,* 160 (2018), pp. 625-634.

[13] Shukla, A. K., Singh, O., Thermodynamic investigation of parameters affecting the execution of steam injected cooled gas turbine based combined cycle power plant with vapor absorption inlet air cooling. *Applied Thermal Engineering,* 122 (2017), pp. 380-388.

[14] Abdel Rahman, A. A., Mokheimer, E. M. A., Boosting Gas Turbine Combined Cycles in Hot Regions Using Inlet Air Cooling including Solar Energy. *Energy Procedia,* 142 (2017), pp. 1509-1515.

[15] Arrieta, F. R. P., Lora, E. E. S., Influence of ambient temperature on combined-cycle power-plant performance, *Applied Energy,* 80 (2005), pp. 261-272.

[16] Akbarpour, G. R., *et al.*, A new approach for optimization of combined cycle system based on first level of exergy destruction splitting, *Sustainable Energy Technologies and Assessments*, 37 (2020), pp. 100600.

[17] Ibrahim, T. K., *et al.*, Thermal performance of gas turbine power plant based on exergy analysis. *Applied Thermal Engineering*, 115 (2017), pp. 977-985.

[18] Mohapatra, A.K., Sanjay, Exergetic evaluation of gas-turbine based combined cycle system with vapor absorption inlet cooling. *Applied Thermal Engineering*, 136 (2018), pp. 431-443.

[19] Kotowicz, J., *et al.*, The thermodynamic and economic characteristics of the modern combined cycle power plant with gas turbine steam cooling. *Energy*, 164 (2018), pp. 359-376.

[20] Kotowicz, J., Brzęczek, M., Analysis of increasing efficiency of modern combined cycle power plant: A case study. *Energy*, 153 (2018), pp. 90-99.

[21] Kwon, H. M., *et al.*, Performance improvement of gas turbine combined cycle power plant by dual cooling of the inlet air and turbine coolant using an absorption chiller. *Energy*, 163 (2018), pp. 1050-1061.

[22] Kurt, H., et al., *Performance analysis of open cycle gas turbine. International Journal of Energy Research*, 33(2009), pp. 285-294.

[23] Alhazmy, M.M. and Najjar, Y.S.H., Augmentation of gas turbine performance using air coolers. *Applied Thermal Engineering*, 24(2004), pp. 415-429.

[24] Ersayin, E., Ozgener, L., Performance analysis of combined cycle power plants: A case study. *Renewable and Sustainable Energy Reviews*, 43 (2015), pp. 832-842.

[25] Ameri, M., *et al.*, 4E analyses and multi-objective optimization of different fuels application for a large combined cycle power plant. *Energy*, 156 (2018), pp. 371-386.

[26] Wang, S., *et al.*, Performance prediction of the combined cycle power plant with inlet air heating under part load conditions. *Energy Conversion and Management*, 200 (2019), pp. 112063.

[27] Wan A. and Chen T., Performance degration analysis of combined cycle power plant under high ambient temperature. *Thermal Science*, Online-First Issue (2021), pp. 226-226.

https://doi.org/10.2298/TSCI210221226W.

Received: 28.06.2021.
Revised: 19.08.2021.
Accepted: 26.08.2021.